

Shock-Tube Measurements of Ignition Delay Times for the Ethane/Dimethyl Ether Blends

Jiaxiang Zhang, Erjiang Hu,* Lun Pan, Zihang Zhang, and Zuohua Huang*

State Key Laboratory of Multiphase Flow in Power Engineering, Xi'an Jiaotong University, Xi'an 710049, People's Republic of China

Supporting Information

ABSTRACT: Ignition delay times of ethane/dimethyl ether (DME) blends (DME blending ratios of 0, 20, 50, and 100%) were studied behind reflected shock waves at pressures of 2.0 and 20.0 atm, temperatures of 1100–1500 K, and equivalence ratios of 0.5, 1.0, and 2.0. Fuel mixtures were prepared with a constant argon dilution ratio for reasonable comparison. Two previous models including both ethane and DME chemistry were used to validate against the measured data. Subsequently, the chemical analysis was performed to obtain insight into the effect of the equivalence ratio and blending ratio on the ignition delay time.

1. INTRODUCTION

Dimethyl ether (DME) is considered to be a very promising alternative fuel for some of its advantages, including high oxygen content, low boiling point, and high cetane number.¹ It has been blended with some hydrocarbon fuels^{2–7} to improve the engine ignition and combustion characteristics. However, only limited fundamental studies^{8–12} on the oxidation of hydrocarbon/DME mixtures were reported. Amano et al.⁸ experimentally studied the effect of the DME blending on the ignition and oxidation of methane under engine conditions in a flow reactor and found that DME is very effective in stimulating the ignition and oxidation of methane. Zinner⁹ measured ignition delay times of DME/methane mixtures in a shock tube over the temperature range of 913–1650 K, pressure range of 0.8–35.7 atm, and equivalence ratios of 0.3, 0.5, 1.0, and 2.0. His results showed that the increase of the DME concentration can accelerate the ignition process at pressures less than 10 atm, while it shows an inhibiting effect on fuel-rich mixtures at pressures higher than 10 atm. Chen et al.¹⁰ measured laminar flame speeds and Markstein lengths of methane/DME–air premixed mixtures to analyze the effect of the DME addition. They found that the laminar flame speed increases almost linearly with the DME addition, while the Markstein length varies remarkably at small DME concentrations. Recently, Tang et al.¹¹ measured ignition delay times of the stoichiometric methane/DME mixtures in a shock tube over the temperature range of 1134–2105 K and pressure range of 1.0–10.0 bar. It is found that ignition delay times of the mixtures dramatically decrease with the presence of only 1% DME. The propane/DME mixtures and *n*-butane/DME mixtures were studied behind reflected shock waves by Hu et al.,^{12,13} who found that ignition delay times of the mixtures decrease almost linearly with increasing the DME blending ratio.

Although some studies have been carried out on the ignition for hydrocarbon/DME blends, ignition delay times of ethane/DME mixtures have not yet been reported. It is well-known that ethane is a major non-methane alkane in natural gas.¹⁴ In addition, ethane presents an anomalous ignition behavior in that it ignites quite faster than all of the other alkanes.^{15–17} Therefore, it is valuable to investigate the effect of the DME addition on the ignition and oxidation of ethane. The measured data are also

important for the validation and improvement of ethane/DME models.

In this study, ignition delay times of ethane/DME blends were tested at pressures of 2.0 and 20.0 atm and equivalence ratios of 0.5, 1.0, and 2.0 over the temperature range of 1100–1500 K. The effect of the equivalence ratio and DME blending ratio was then analyzed by chemical kinetic modeling.

2. EXPERIMENTAL SECTION

The measurements were carried out in a shock tube with a diameter of 11.5 cm. The respective lengths of the driver and driven sections are 4.0 and 5.3 m. The detailed introduction of this shock tube was mentioned in another study.¹⁸

In this study, the purities of ethane and DME are higher than 99.9 and 99.5%, respectively. Other used gases, including oxygen, argon, and

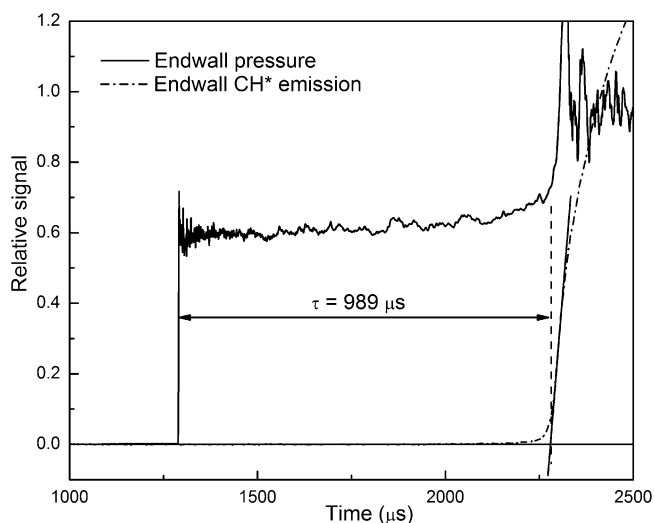


Figure 1. Typical definition of the ignition delay time for neat ethane at $T = 1165$ K, $p = 20.74$ atm, and $\phi = 1.0$.

Received: July 8, 2013

Revised: September 7, 2013

Published: September 8, 2013

Table 1. List of Fuel Mixtures in This Study

mixtures	ϕ	ethane (%)	DME (%)	O ₂ (%)	Ar (%)
DME0	0.5	0.58	0	4.08	95.34
DME20	0.5	0.48	0.12	4.07	95.33
DME50	0.5	0.31	0.31	4.07	95.31
DME100 ^a	0.5	0	0.68	4.06	95.26
DME0	1.0	1.13	0	3.96	94.91
DME50	1.0	0.61	0.61	3.95	94.83
DME100 ^a	1.0	0	1.31	3.93	94.76
DME0	2.0	2.14	0	3.75	94.11
DME100 ^a	2.0	0	2.46	3.68	93.86

^aIgnition delay times of DME100 have been measured in the literature.¹²

helium, are of the same purity of 99.999%. Helium was used as the driver gas. A 128L stainless-steel tank was used to prepare fuel mixtures. The fuel component was charged to the tank manometrically. A typical definition of the ignition delay time is shown in Figure 1. The start of the ignition delay is the arrival of the incident shock wave at the endwall. The onset of the ignition is the intersection of the zero baseline and the extrapolation at the maximum rise of the endwall CH* signal. The CH* signal is detected by a photomultiplier (Hamamatsu, CRI31) located at the endwall. To obtain the incident shock velocity, three time counters (Fluke, PM6699) are used to record the intervals between four pressure transducers (PCB, 113B26) located at the sidewall of the tube. Three incident shock velocities can be obtained on the basis of the time intervals and the constant distances of the pressures. Then, the incident shock velocity at the endwall is determined by extrapolating the above three shock velocities. Finally, the incident shock velocity is used to calculate the temperature behind reflected shock waves by employing the software Gaseq.¹⁹ The pressure behind reflected shock waves is directly measured by the endwall pressure transducer.²⁰

The ethane/DME/oxygen/argon mixtures ($\phi = 0.5, 1.0, \text{ and } 2.0$ and $X_{\text{O}_2}/X_{\text{Ar}} = 21:79$) were further diluted with argon (20% mixture/80%

argon), as shown in Table 1. The dilution method was also employed in the literature.^{11,15} Ignition delay times of neat DME¹¹ and neat ethane¹⁷ have been measured using this shock tube and agree fairly well with previous studies. It gives us confidence to conduct the ignition measurements of ethane/DME mixtures. Table 2 gives all of the measured data in the study.

Simulations of ignition delay times were conducted using Senkin²¹ in the Chemkin II package.²² The ignition delay time is obtained from the simulation results as the time interval between zero and the maximum rate of the temperature rises (maximum dT/dt).

3. RESULTS AND DISCUSSION

3.1. Measured and Calculated Ignition Delay Times.

Two models, the AramcoMech_1.3²³ model and Zhao's model,²⁴ were employed for simulation. The AramcoMech_1.3 model has been updated recently and validated against C₁–C₂ hydrocarbon and oxygenated fuel data. Zhao's model mainly focuses on the oxidation of DME, but it also contains the detailed C₀–C₂ chemistry. The pressure rise in the shock-tube measurement exerts a considerable effect on relatively longer ignition delay times. The Hanson group developed a CHEMSHOCK model²⁵ to consider the effect of the pressure rise. Later, Chaos et al.²⁶ proposed the variable volume method (VTIM) to achieve the same target. The ignition delay time is up to 3.0 ms in this study. The VTIM method was employed with a pressure rise of 4%/ms, which has been experimentally measured in the study.²⁷

Figures 2 and 3 show the comparison between measured and calculated ignition delay times using two models. At the fuel-lean case ($\phi = 0.5$), neat ethane shows quite shorter ignition delay times than those of the neat DME mixture at two specified pressures. With the increase of the DME blending ratio, ignition delay times of fuel mixtures become longer. At stoichiometric and fuel-rich cases ($\phi = 1.0$ and 2.0), ignition delay times of

Table 2. Measured Ignition Delay Times of Ethane/DME Blends

fuel	p (atm)	T (K)	τ (μ s)	fuel	p (atm)	T (K)	τ (μ s)	fuel	p (atm)	T (K)	τ (μ s)
	$\phi = 0.5$				$\phi = 1.0$				$\phi = 2.0$		
DME0	2.00	1298	280	DME20	2.18	1201	980	DME0	21.04	1251	284
	2.03	1231	610		2.00	1145	2712		20.74	1165	989
	1.96	1250	433		2.07	1222	891		20.88	1322	114
	1.91	1144	1753		21.09	1227	454		21.44	1418	44
	2.06	1211	811		20.52	1136	1628		22.07	1242	335
	2.02	1184	1021		21.46	1206	593		21.31	1118	1716
	2.02	1384	136		21.61	1329	139	DME50	21.90	1245	433
	2.01	1346	201		20.09	1236	415		21.10	1165	969
	2.02	1422	112		21.14	1297	166		21.87	1139	1370
	2.06	1470	81		21.26	1179	856		20.60	1306	205
	1.99	1472	75		21.96	1420	48		21.57	1411	66
	1.93	1479	88	DME50	1.99	1417	153		20.63	1332	154
	20.86	1216	396		2.03	1371	265		19.81	1146	855
	20.71	1141	1410		1.99	1291	673		$\phi = 2.0$		
	20.42	1168	820		1.93	1213	1617	DME0	20.33	1170	858
	21.37	1281	169		2.00	1264	894		20.83	1259	410
	19.50	1250	182		2.07	1256	993		21.53	1153	993
	20.49	1289	146		1.97	1319	412		20.44	1071	2470
	21.35	1360	60		21.90	1245	433		20.41	1311	256
DME20	2.06	1466	80		21.10	1165	969		21.05	1406	131
	2.05	1393	148		21.87	1139	1370				
	2.06	1328	270		20.60	1306	205				
	2.07	1262	548		21.57	1411	66				
	2.09	1196	1194		20.63	1332	154				
	2.03	1137	2085		19.81	1146	855				

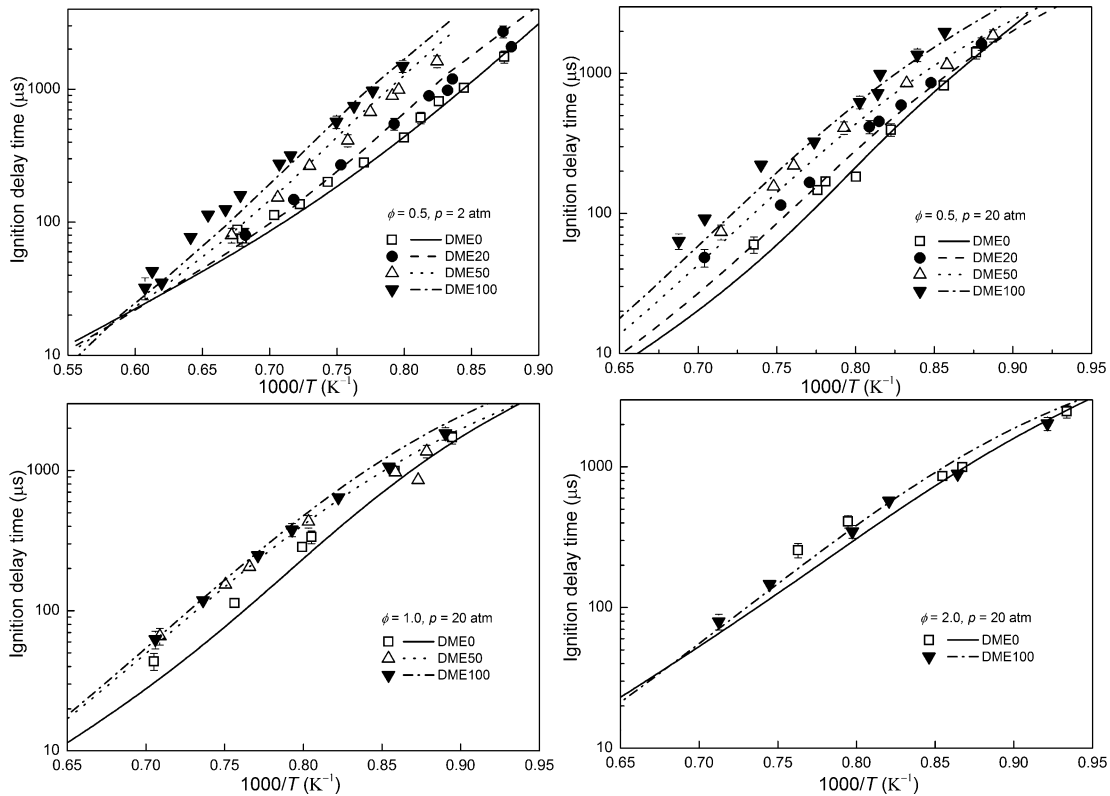


Figure 2. Comparison between measured and simulated ignition delay times by the AramcoMech_1.3 model.

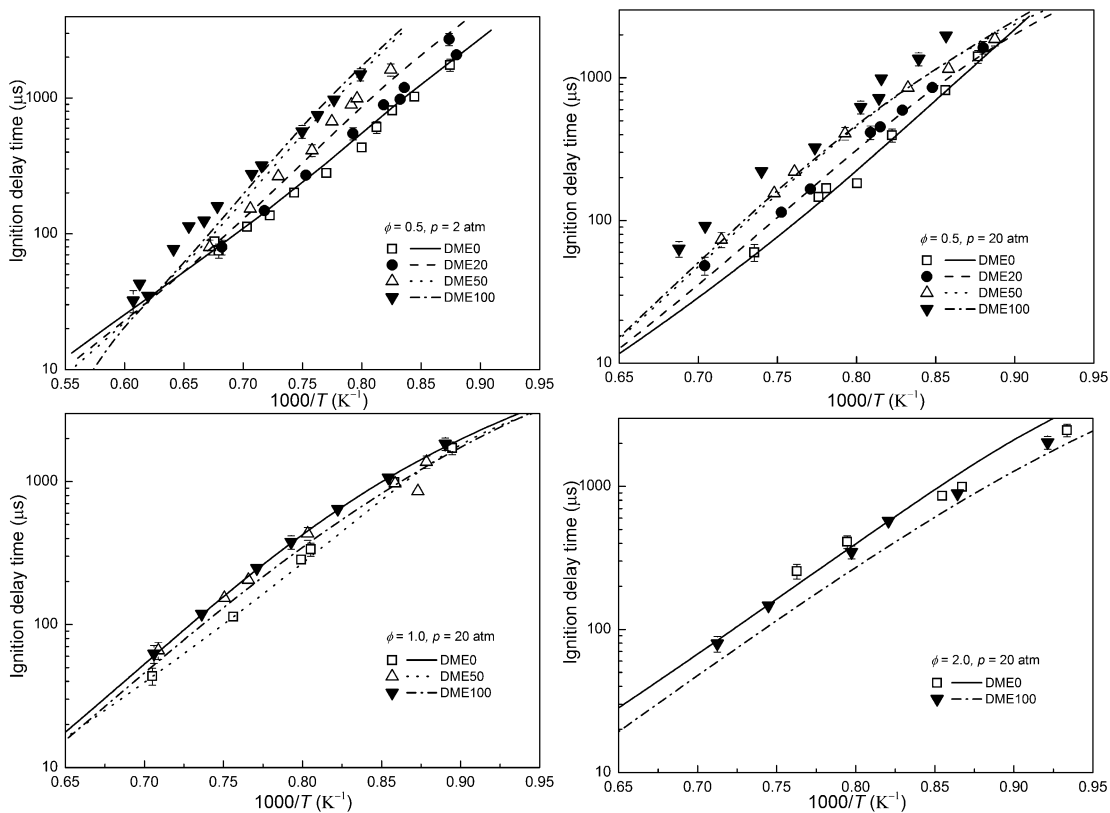


Figure 3. Comparison between measured and calculated ignition delay times by Zhao's model.

ethane/DME mixtures were only measured at $p = 20$ atm. It is found that, in comparison to the fuel-lean case, neat ethane and neat DME present relatively close ignition delay times.

Particularly, two neat fuels nearly overlap with each other at $\phi = 2.0$. In general, the effect of the DME addition is more remarkable under fuel-lean conditions.

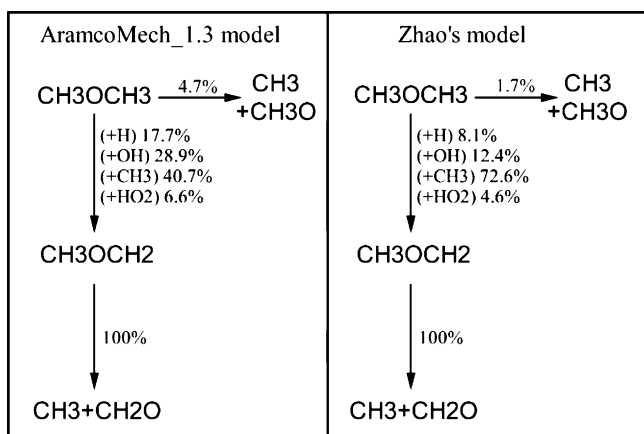


Figure 4. Reaction pathway analysis of two models at $T = 1200$ K, $p = 20$ atm, $\phi = 2.0$, and 20% DME consumption.

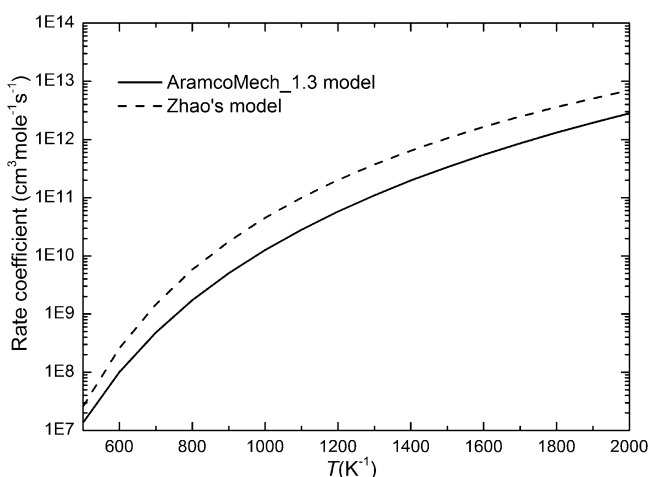


Figure 5. Comparison of rate constants of the reaction ($\text{CH}_3\text{OCH}_3 + \text{CH}_3 \rightleftharpoons \text{CH}_3\text{OCH}_2 + \text{CH}_4$) in the two models.

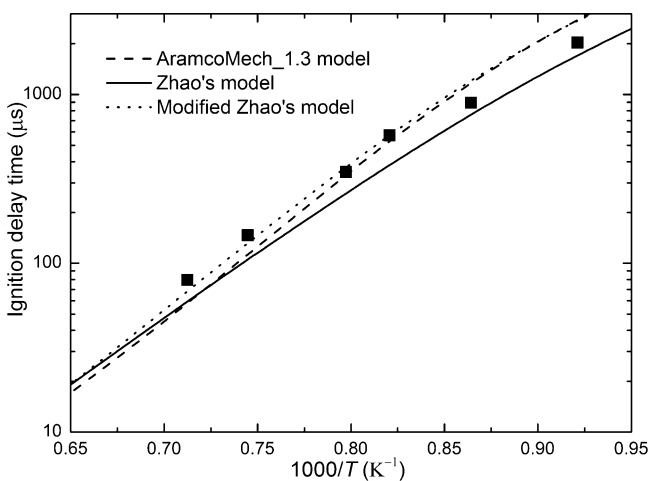


Figure 6. Effect of the reaction ($\text{CH}_3\text{OCH}_3 + \text{CH}_3 \rightleftharpoons \text{CH}_3\text{OCH}_2 + \text{CH}_4$) on Zhao's model.

Validations of the AramcoMech_1.3 model and Zhao's model against the experimental data are also shown in Figures 2 and 3, respectively. The AramcoMech_1.3 model yields fairly good agreements not only with neat fuels both also with their mixtures under all test conditions. At $\phi = 0.5$, Zhao's model yields fairly

good agreement with neat ethane and neat DME at $p = 2.0$ atm, but it notably overpredicts the ignition values by 10–30% for DME20 and DME50. However, at $p = 20.0$ atm, about 20–50% underprediction for neat DME occurs at three different equivalence ratios. Therefore, the modeling ignition delay times of DME50 are even longer than those of neat DME at $\phi = 1.0$. At $\phi = 2.0$, the modeling ignition delay times of neat ethane are also longer than those of neat DME.

Because Zhao's model shows relatively poor prediction under fuel-rich conditions, reaction pathway analysis of the two models was conducted at $T = 1200$ K, $p = 20$ atm, and $\phi = 2.0$ to ascertain the controlling steps. As shown in Figure 4, H-abstraction by CH_3 radicals is the dominated pathway consuming DME in both models, especially in Zhao's model. It is because the decomposition of DME and CH_3OCH_2 radicals produces abundant CH_3 radicals to feed H-abstraction. Therefore, it is quite possible that the different rate constants of the reaction ($\text{CH}_3\text{OCH}_3 + \text{CH}_3 \rightleftharpoons \text{CH}_3\text{OCH}_2 + \text{CH}_4$) in the two models contribute to their different predictions. Figure 5 shows the comparison of the reaction in these two models. It is observed that the rate constant in Zhao's model is about 2 times higher than that in the AramcoMech_1.3 model. Then, the rate constant of this elementary reaction in Zhao's model was replaced by the rate constant in the AramcoMech_1.3 model to identify the influence of this reaction. As shown in Figure 6, the modified Zhao's model shows fairly better agreement with the experimental data than the original Zhao's model. Other main pathways were also examined and exert little influence on Zhao's model. Considering that rate constants of this elementary reaction in these two models are roughly estimated by respective authors, experiment or high-level calculation for this rate constant is suggested to further improve the accuracy of the DME kinetics.

The comparison shows that the AramcoMech_1.3 model gives better prediction on ethane/DME blends than Zhao's model. Thus, the AramcoMech_1.3 model is used for the chemical analysis in the following sections.

3.2. Effect of the Equivalence Ratio. As observed in Figure 2, ignition delay times of DME/ethane mixtures under the fuel-lean conditions present quite large variation compared to those under the stoichiometric and fuel-rich conditions. To ascertain the effect of the equivalence ratio, ignition delay times of neat ethane and neat DME under various equivalence ratios are compared in panels a and b of Figure 7, respectively. It is observed that ignition delay times of neat ethane increase with the increase of the equivalence ratio at most temperatures. On the contrary, ignition delay times of neat DME decrease with the increase of the equivalence ratio. In addition, neat ethane and neat DME show comparable ignition delay times at the fuel-rich case ($\phi = 2.0$), as shown in Figure 2. Therefore, with decreasing the equivalence ratio, ignition delay times of neat ethane become shorter, while those of neat DME become longer, leading to the quite large variation of neat ethane and neat DME at $\phi = 0.5$.

To further study the different effects of the equivalence ratio on neat ethane and neat DME, the ignition sensitivity analysis was performed at $p = 20$ atm, $T = 1300$ K, and $\phi = 0.5$, as shown in Figure 8. The sensitivity is defined as

$$S = \frac{\tau(2k_i) - \tau(0.5k_i)}{1.5\tau(k_i)} \quad (1)$$

where k_i is the pre-exponential factor of the i th reaction and τ is the ignition delay time. For neat ethane in Figure 8a, the ignition

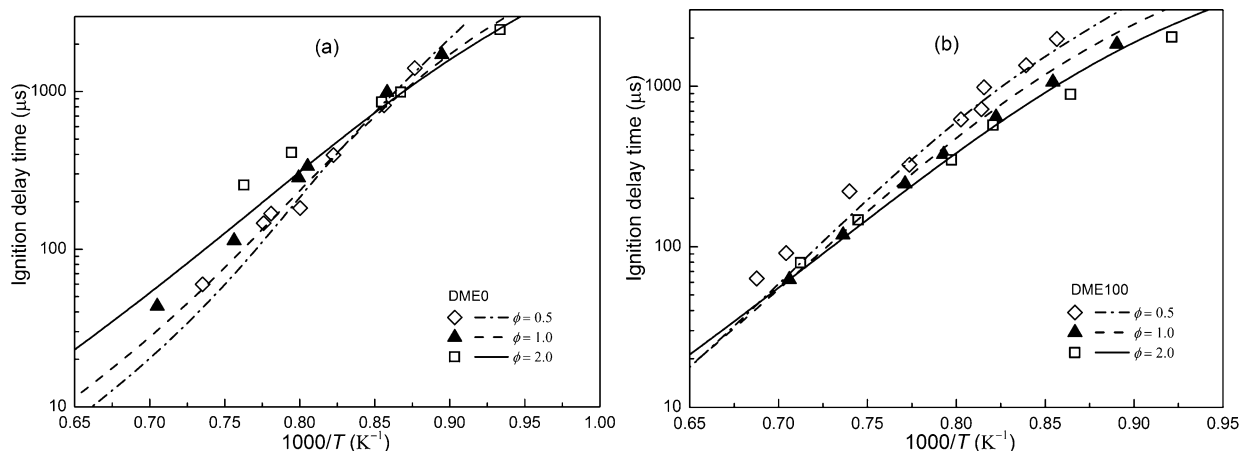


Figure 7. Effect of the equivalence ratio on (a) neat ethane (DME0) and (b) neat DME (DME100) at $p = 20$ atm.

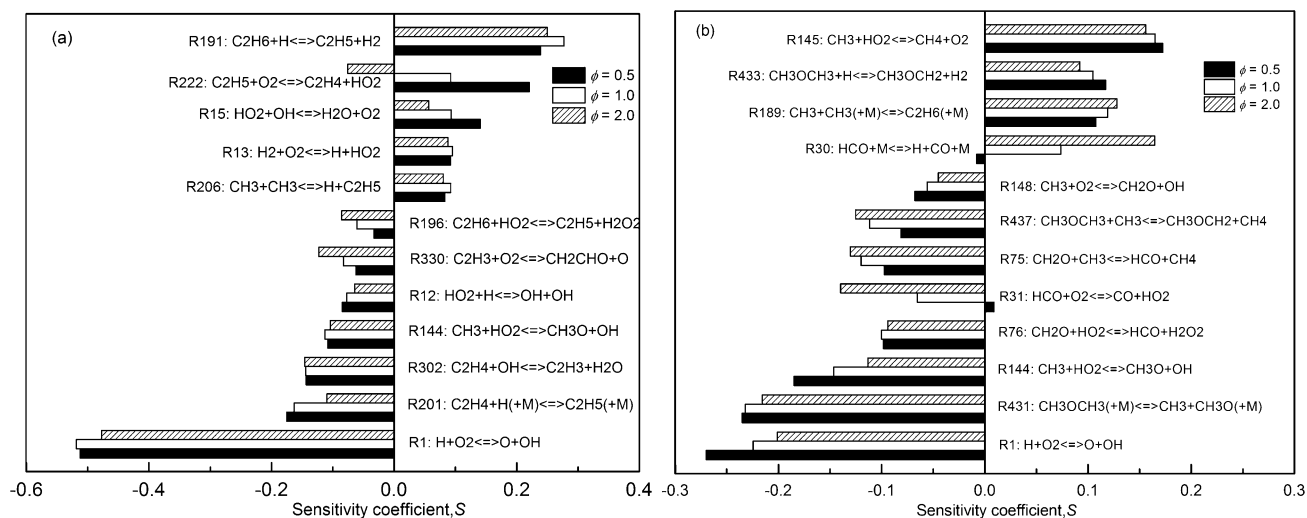


Figure 8. Sensitivity analysis for (a) neat ethane and (b) neat DME at $T = 1300$ K, $p = 20$ atm, and $\phi = 0.5$.

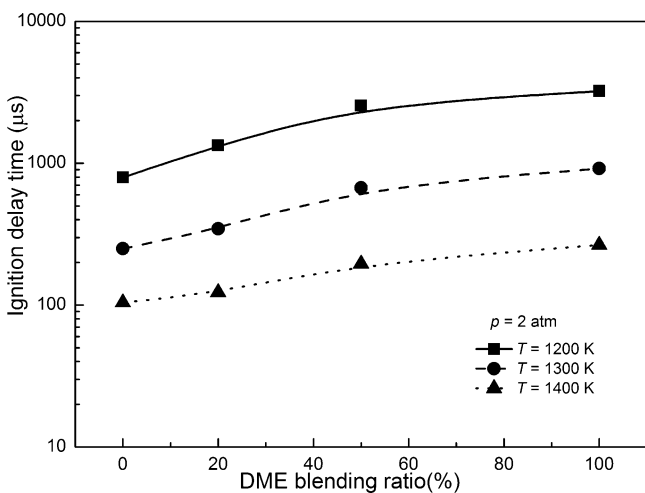


Figure 9. Ignition delay times versus DME blending ratio.

delay time shows extremely high sensitivity to the reaction R1 ($H + O_2 \rightleftharpoons O + OH$). Therefore, in comparison to the fuel-rich mixture, the fuel-lean mixture has a higher oxygen concentration, leading to a higher reaction rate of reaction R1 and shorter ignition delay times. However, although the ignition delay time of neat DME is also sensitive to reaction R1, the fuel-specific

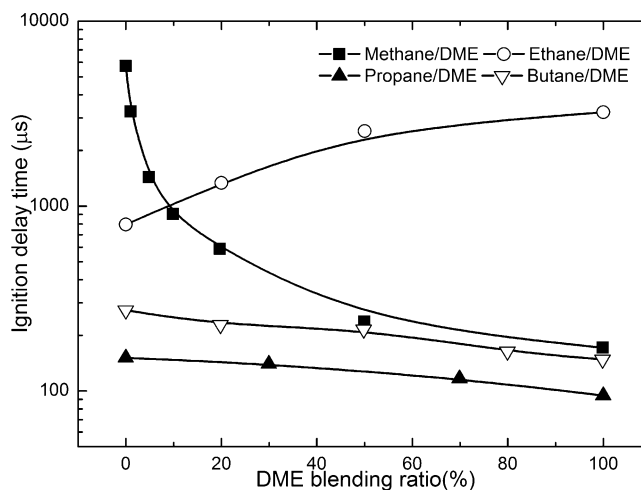


Figure 10. Ignition delay times versus the DME blending ratio for four hydrocarbon/DME blends (methane/DME,¹¹ $T = 1500$ K, $p = 1$ atm, and $\phi = 1.0$; ethane/DME, $T = 1200$ K, $p = 2$ atm, and $\phi = 0.5$; propane/DME,¹² $T = 1500$ K, $p = 1.2$ atm, and $\phi = 1.0$; and butane/DME,¹³ $T = 1500$ K, $p = 20$ atm, and $\phi = 1.0$).

reactions R431 [$CH_3OCH_3 (+M) \rightleftharpoons CH_3 + CH_3O (+M)$] and R437 ($CH_3OCH_3 + CH_3 \rightleftharpoons CH_3OCH_2 + CH_4$) also show quite

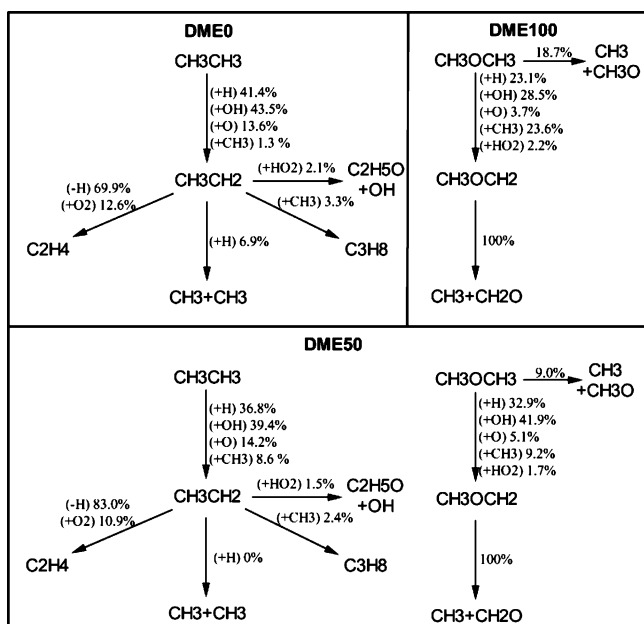


Figure 11. Reaction pathways for three fuel mixtures (DME0, DME50, and DME100) at $T = 1200$ K, $p = 2$ atm, $\phi = 0.5$, and 20% fuel consumption.

high sensitivity, as shown in Figure 8b. Because of the higher fuel concentration in the fuel-rich mixture, reactions R431 and R437 have higher reaction rates under the fuel-rich condition. Therefore, ignition delay times of neat DME decrease with the increase of the equivalence ratio.

3.3. Effect of the DME Blending Ratio. Because ignition delay times of ethane/DME blends vary remarkably with the variation of the DME blending ratio under the fuel-lean conditions, the effect of the DME blending ratio is analyzed at $\phi = 0.5$. Figure 9 shows the variation of ignition delay times versus the DME blending ratio at three different temperatures. It is noted that ignition correlations cannot be developed because the measured data do not show complete Arrhenius temperature dependence. In addition, it is difficult to obtain the experimental data points at the same temperature for various mixtures. As a result, modeling results by the AramcoMech_1.3 model are used for comparison. It is found that ignition delay times of ethane/DME mixtures increase nonlinearly with increasing the DME blending ratio, especially at $T = 1200$ K. In comparison to the very slow increase for DME-rich mixtures, ignition delay times increase fast at DME blending ratios less than 50%. Figure 10 shows ignition delay times of four hydrocarbon/DME blends versus the DME blending ratio. Although the comparison was conducted under different experimental conditions, the data can represent the respective ignition characteristics of four blends. It is observed that ethane/DME blends show quite different ignition behaviors from the other three hydrocarbon/DME blends. With the increase of the DME blending ratio, ignition delay times of methane/DME¹¹ blends decrease nonlinearly and sharply, while those of propane/DME¹² and *n*-butane/DME¹³ blends decrease linearly.

To further understand the effect of the DME blending ratio, reaction pathways of neat ethane (DME0), the ethane/DME mixture (DME50), and neat DME (DME100) were analyzed at $T = 1200$ K, $p = 2.0$ atm, and $\phi = 0.5$, as shown in Figure 11. The timing at 20% fuel consumption is selected according to the

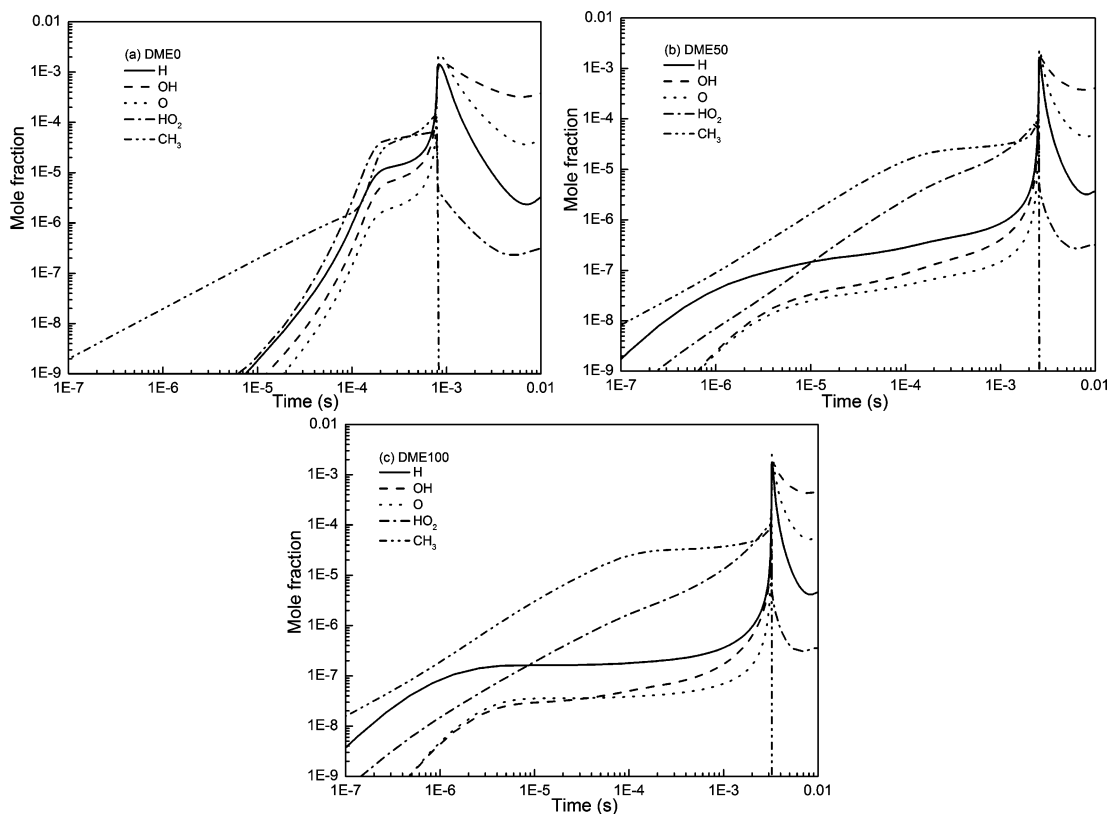


Figure 12. Mole fraction of small radicals (H, OH, O, HO₂, and CH₃) for three fuel mixtures (a, DME0; b, DME50; and c, DME100) at $T = 1200$ K, $p = 2$ atm, and $\phi = 0.5$.

previous literature.¹⁷ It is noted that, for DME50, the analysis was conducted at the timing of 20% ethane consumption because of the different consumption rates of ethane and DME. Figure 12 presents mole fractions of small radicals (H, OH, O, HO₂, and CH₃) for the three mixtures under the same condition.

For neat ethane shown in Figure 11, most ethane undergoes H-abstraction by the small radicals (H, OH, O, and CH₃) to form ethyl radicals. Subsequently, 69.9% ethyl radicals decompose to produce ethene and H radicals, resulting in the very fast increase of H radicals of neat ethane in Figure 8a. The abundant H radicals then produce much OH and O radicals by reaction R1 ($H + O_2 \rightleftharpoons OH + O$). A total of 6.9% of ethyl radicals react with H to form methyl radicals, resulting in the relatively fast increase of methyl radicals in Figure 12a.

Only 18.7% of neat DME directly decomposes to form methyl and CH₃O radicals, while most DME undergoes H-abstraction by the small radicals to form CH₃OCH₂. Subsequently, the produced CH₃OCH₂ radicals decompose to form methyl radical and formaldehyde. The decomposition of DME and CH₃OCH₂ radicals is ascribed to the very high mole fraction of methyl radicals for the neat DME mixture in Figure 12c. In the oxidation of neat DME, H radicals are mainly produced by a small amount of CH₃O radicals by reaction [$CH_3O (+M) \rightleftharpoons CH_2O + H (+M)$], leading to their relatively slow increase.

For DME50 shown in Figure 12b, all small radicals show similar profiles to those of neat DME but they have slightly higher values than those of neat DME and quite lower values than those of neat ethane. Thus, the addition of 50% DME to ethane greatly changes the mole fractions of small radicals, leading to the fast increase of ignition delay times, as shown in Figure 9. In the oxidation of DME50 in Figure 11, the reaction pathway ($C_2H_5 + H \rightleftharpoons CH_3 + CH_3$) is completely shutdown because of the very high mole fraction of methyl radicals mainly produced by the DME component. In comparison to neat DME, H-abstractions by H, O, and OH radicals have higher branching ratios. These H, O, and OH radicals are partly derived from the oxidation of the ethane component. Therefore, although ethane can produce H, O, and OH radicals more readily than DME, the produced H radicals by ethane feed not only ethane itself but also DME for H-abstraction in the oxidation of DME50. As a result, the reaction rate of ethane in the oxidation of DME50 is greatly reduced, leading to the great increase of ignition delay times.

4. CONCLUSION

Ignition delay times of ethane/DME mixtures were measured in a shock tube. The AramcoMech_1.3 model and Zhao's model were employed for the simulation of the ignition delay time. The AramcoMech_1.3 model well captures the effect of the DME blending ratio on ignition delay times of ethane/DME mixtures and yields good agreements with measurements under all test conditions. Zhao's chemical model yields remarkable under-prediction for DME-rich mixtures, which is probably caused by the too high reaction rate of reaction ($CH_3OCH_3 + CH_3 \rightleftharpoons CH_3OCH_2 + CH_4$). With increasing the equivalence ratio, ignition delay times of neat ethane increase, while those of neat DME decrease. The DME blending ratio shows a nonlinear effect on the ignition delay time because of the competition of DME for small radicals produced by ethane.

■ ASSOCIATED CONTENT

Supporting Information

Uncertainty analysis of the temperature behind reflected shock waves and comparison to other shock-tube facilities. This

material is available free of charge via the Internet at <http://pubs.acs.org>.

■ AUTHOR INFORMATION

Corresponding Authors

*Telephone: 0086-29-82665075. Fax: 0086-29-82668789. E-mail: huijiang@mail.xjtu.edu.cn.

*Telephone: 0086-29-82665075. Fax: 0086-29-82668789. E-mail: zhhuang@mail.xjtu.edu.cn.

Notes

The authors declare no competing financial interest.

■ ACKNOWLEDGMENTS

The study is supported by the National Natural Science Foundation of China (51306144 and 51136005), the National Basic Research Program (2013CB228406), and the Ministry of Education of China (20110201120045). The support from the State Key Laboratory of Engines (SKLE201302) and the Fundamental Research Funds for the Central Universities is also appreciated.

■ REFERENCES

- (1) Arcoumanis, C.; Bae, C.; Crookes, R.; Kinoshita, E. The potential of di-methyl ether (DME) as an alternative fuel for compression-ignition engines: A review. *Fuel* **2008**, *87*, 1014–1030.
- (2) Jeon, J.; Bae, C. The effects of hydrogen addition on engine power and emission in DME premixed charge compression ignition engine. *Int. J. Hydrogen Energy* **2013**, *38*, 265–273.
- (3) Kong, S. C. A study of natural gas/DME combustion in HCCI engines using CFD with detailed chemical kinetics. *Fuel* **2007**, *86*, 1483–1489.
- (4) Tsutsumi, Y.; Iijima, A.; Yoshida, K.; Shoji, H.; Lee, J. T. HCCI combustion characteristics during operation on DME and methane fuels. *Int. J. Automot. Technol.* **2009**, *10*, 645–652.
- (5) Takatsuto, R.; Igarashi, T.; Iida, N. Auto ignition and combustion of DME and *n*-butane/air mixtures in homogeneous charge compression ignition engine. *COMODIA 98: Proceedings of the 4th International Symposium on Diagnostics and Modeling of Combustion in Internal Combustion Engines*; Kyoto International Conference Hall, Kyoto, Japan, July 20–23, 1998; pp 185–190.
- (6) Lee, S.; Oh, S.; Choi, Y. Performance and emission characteristics of an SI engine operated with DME blended LPG fuel. *Fuel* **2009**, *88*, 1009–1015.
- (7) Lee, S.; Oh, S.; Choi, Y.; Kang, K. Effect of *n*-butane and propane on performance and emission characteristics of an SI engine operated with DME-blended LPG fuel. *Fuel* **2011**, *90*, 1674–1680.
- (8) Amano, T.; Dryer, F. L. Effect of dimethyl ether, NO_x, and ethane on CH₄ oxidation: high pressure, intermediate-temperature experiments and modeling. *Proc. Combust. Inst.* **1998**, *27*, 397–404.
- (9) Zinner, C. M. Methane and dimethyl ether oxidation at elevated temperatures and pressure. Master's Thesis, University of Central Florida, Orlando, FL, 2006.
- (10) Chen, Z.; Qin, X.; Ju, Y.; Zhao, Z.; Chaos, M.; Dryer, F. L. High temperature ignition and combustion enhancement by dimethyl ether addition to methane–air mixtures. *Proc. Combust. Inst.* **2007**, *31*, 1215–1222.
- (11) Tang, C.; Wei, L.; Zhang, J.; Man, X.; Huang, Z. Shock tube measurements and kinetic investigation on the ignition delay times of methane/dimethyl ether mixtures. *Energy Fuels* **2012**, *26*, 6720–6728.
- (12) Hu, E.; Zhang, Z.; Pan, L.; Zhang, J.; Huang, Z. Experimental and modeling study on ignition delay times of dimethyl ether/propane/O₂/Ar mixtures at 20 bar. *Energy Fuels* **2013**, *27*, 4007–4013.
- (13) Hu, E.; Jiang, X.; Huang, Z.; Zhang, J.; Zhang, Z.; Man, X. Experimental and kinetic studies on ignition delay times of dimethyl ether/*n*-butane/O₂/Ar mixtures. *Energy Fuels* **2013**, *27*, 530–536.

- (14) Huang, J.; Bushe, W. Experimental and kinetic study of autoignition in methane/ethane/air and methane/propane/air mixtures under engine-relevant conditions. *Combust. Flame* **2006**, *144*, 74–88.
- (15) Burcat, A.; Scheller, K.; Lifshitz, A. Shock-tube investigation of comparative ignition delay times for C_1 – C_5 alkanes. *Combust. Flame* **1971**, *16*, 29–33.
- (16) Westbrook, C. K.; Mizobuchi, Y.; Poinso, T. J.; Smith, P. J.; Warnatz, J. Computational combustion. *Proc. Combust. Inst.* **2005**, *30*, 125–157.
- (17) Zhang, J.; Hu, E.; Zhang, Z.; Pan, L.; Huang, Z. Comparative study on ignition delay times of C_1 – C_4 alkanes. *Energy Fuels* **2013**, *27*, 3480–3487.
- (18) Zhang, J.; Wei, L.; Man, X.; Jiang, X.; Zhang, Y.; Hu, E.; Huang, Z. Experimental and modeling study of *n*-butanol oxidation at high temperature. *Energy Fuels* **2012**, *26*, 3368–3380.
- (19) Morley, C. *Gaseq, Version 0.76*; <http://www.gaseq.co.uk>.
- (20) Jiang, X.; Zhang, Y.; Man, X.; Pan, L.; Huang, Z. Shock tube measurements and kinetic study on ignition delay times of lean DME/*n*-butane blends at elevated pressures. *Energy Fuels* **2013**, DOI: 10.1021/ef401252e.
- (21) Lutz, A. E.; Kee, R. J.; Miller, J. A. *SENKIN: A Fortran Program for Predicting Homogeneous Gas Phase Chemical Kinetics with Sensitivity Analysis*; Sandia National Laboratories: Albuquerque, NM, 1988; SAND87-8248.
- (22) Kee, R. J.; Rupley, F. M.; Miller, J. A. *CHEMKIN-II: A Fortran Chemical Kinetics Package for the Analysis of Gas-Phase Chemical Kinetics*; Sandia National Laboratories: Albuquerque, NM, 1989; SAND89-8009.
- (23) Metcalfe, W. K.; Burke, S. M.; Ahmed, S. S.; Curran, H. J. A hierarchical and comparative kinetic modeling study of C_1 – C_2 hydrocarbon and oxygenated fuels. *Int. J. Chem. Kinet.* **2013**, *45*, 638–675.
- (24) Zhao, Z.; Chaos, M.; Kazakov, A.; Dryer, F. L. Thermal decomposition reaction and a comprehensive kinetic model of dimethyl ether. *Int. J. Chem. Kinet.* **2008**, *40*, 1–18.
- (25) Li, H.; Owens, Z. C.; Davidson, D. F.; Hanson, R. K. A simple reactive gasdynamic model for the computation of gas temperature and species concentrations behind reflected shock waves. *Int. J. Chem. Kinet.* **2008**, *40*, 189–198.
- (26) Chaos, M.; Dryer, F. L. Chemical-kinetic modeling of ignition delay: Considerations in interpreting shock tube data. *Int. J. Chem. Kinet.* **2010**, *42*, 143–150.
- (27) Zhang, Y.; Huang, Z.; Wei, L.; Zhang, J.; Law, C. K. Experimental and modeling study on ignition delays of lean mixtures of methane, hydrogen, oxygen, and argon at elevated pressures. *Combust. Flame* **2012**, *159*, 918–931.